

S.1 Fabrication process for PDMS microfluidic channels with multilayered design

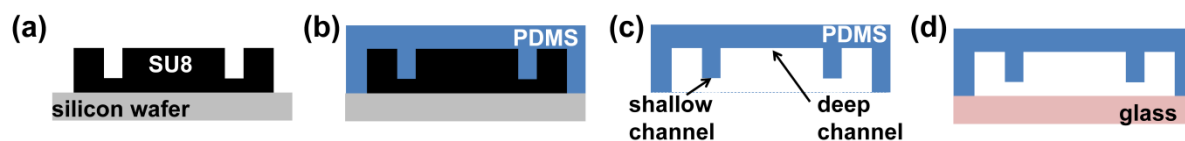


Fig. S1 Scheme of the fabrication process for PDMS microfluidic channels with multilayered design.

Fig. S1(a) - (d) shows schematic diagrams that describe the procedures for fabricating microfluidic devices with multilayered design. We fabricated microfluidic chips using the standard soft lithography: (a) A 4-inch silicon wafer was spin-coated with negative photoresist (SU-8 2005, MicroChem Inc., target: 5 μm), and then the coated silicon wafer was soft-baked for several minutes. The wafer was exposed under a mask using an aligner and placed on a hot-plate for several minutes of post-exposure baking, followed by a short relaxation time. Post-exposure baking was followed by development at room temperature, after which the whole wafer was rinsed with isopropyl alcohol (IPA) to clean the residues from the wafer. Subsequently, SU-8 2050 was patterned on the first SU-8 layer (target: 100 μm , this layer is for the deep channel) with same process as above. (b) A Polydimethylsiloxane (PDMS) precursor (Sylgard 184 Silicone Elastomer, Dow Corning) and a curing agent were mixed at a ratio of 10 to 1, based on weight. Before the PDMS mixture was poured onto the fabricated master, the master was silanized with (tridecafluoro-1,1,2,2,-tetrahydrooctyl)-1-trichlorosilane (Sigma Chemical Co., St. Louis, MO, USA) to allow easier removal of the PDMS after curing. The PDMS mixture was poured onto the master and cured at 95 $^{\circ}\text{C}$ for 1 h. (c) Then, the cured PDMS channel was peeled off from the master, cut and punched to connect microtubes. (d) The PDMS devices were directly bonded to a glass substrate without any surface treatment and then they were treated with oxygen plasma under 50 sccm of O_2 and 70 W for 40 s (Cute-MP, Femto Science, Korea).

S.2 Calibration between fluorescent intensity versus cell density

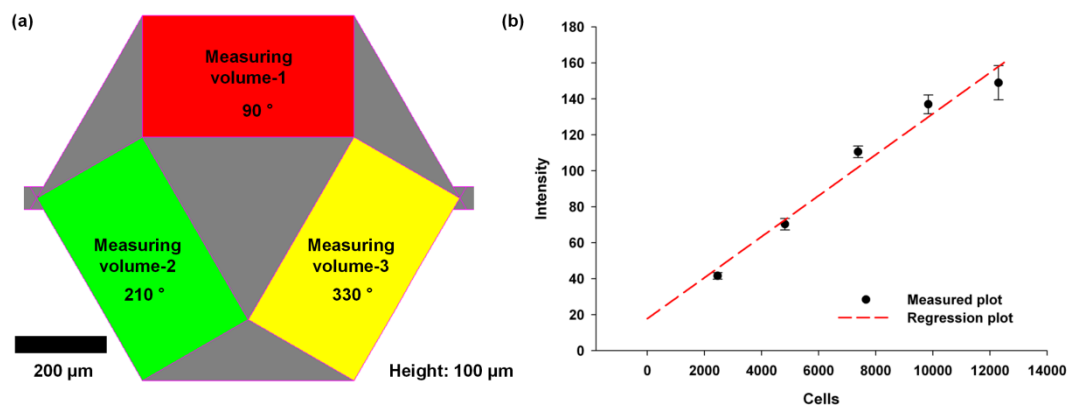


Fig. S2 (a) Schematic illustration of the measuring volume. (b) Measured scatter plots and regression plots of the calibration results between fluorescent intensity versus cell count

Table S1. Calibration results between fluorescent intensity versus cell count

Cell concentration ^a [normalized value]	Fluorescent intensity ^b [AU]	Cells in 10 μl drop ^c [cells]	Cells in measuring volume ^d [cells]
1.0	137.60 ± 22.47	1.0 × 10 ⁷	1.23 × 10 ⁴
0.8	131.59 ± 12.09	0.8 × 10 ⁷	9.84 × 10 ³
0.6	107.57 ± 7.03	0.6 × 10 ⁷	7.38 × 10 ³
0.4	68.19 ± 6.90	0.4 × 10 ⁷	4.82 × 10 ³
0.2	40.68 ± 4.47	0.2 × 10 ⁷	2.46 × 10 ³

^aThe normalized cell concentration was controlled by added the M9 medium into the OD₆₀₀ = 1.0 with volume ratio.

^b10 μl drop of cells were loaded into the reservoir with 900 μm diameter and the fluorescent intensity was averaged over all area. The 10 × objective lens was used and expose time was 900 ms.

^cApproximately, 10⁹ cells/mL is exist in OD₆₀₀ = 1.

^dIn all experiments, the cell was counted at each three volume where the chemical concentration was generated (90°, 210°, and 330°). These measuring volumes are depicted in Fig. S2 (a) and its value is 1.23 × 10⁷ μm³.

$$\text{Cells in measuring volume [cells]} = \text{Cells in 10 } \mu\text{l drop [cells]} \times \frac{\text{Measuring volume}}{\text{Drop volume}}$$

As shown in Fig. S2 (b), the linear regression could be plot based on this calibration table and cell count which was depended on fluorescent intensity measured by using cells expressing GFP was derived as below equation:

$$\text{Cells in measuring volume [cells]} = \frac{\text{Fluorescent intensity} - 17.7967}{0.0113928}$$

S.3 Decay in fluorescent intensity along the membrane

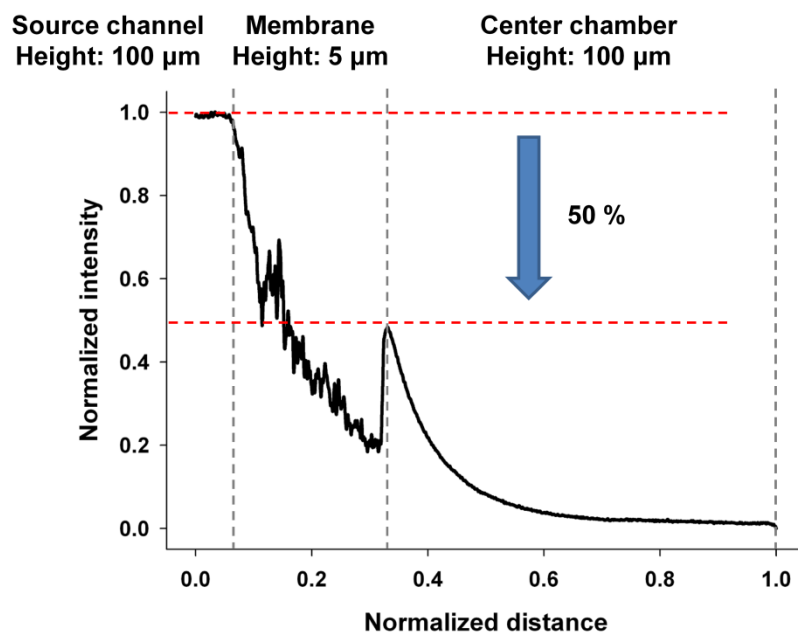


Fig. S3 Decrease of normalized fluorescence intensity through the membrane.

As shown in Fig. S3, when we used the FITC (MW 389, $0.49 \times 10^{-9} \text{ m}^2/\text{s}$), the normalized fluorescence intensity was decreased along the membrane and approximately, there was 50 % of intensity gap between source channel and center chamber after 1 hour.

S.4 Theoretical solution

The theoretical profile (red line) of fluorescence evolution in Fig. 3(f) was obtained from the time-dependent (t) solution of the diffusion equation in two-dimension.¹ The diffusion equation in orthogonal coordinate can be expressed as follows:

$$\frac{\partial C}{\partial t} = D \left(\frac{\partial^2 C}{\partial x^2} + \frac{\partial^2 C}{\partial y^2} \right) \quad (1)$$

where C is the concentration of the diffusing molecule and D is the diffusion coefficient. However, in our proposed device, since the chemical molecules were diffused through the radial direction, it is more practical to use a circular cylindrical coordinate. The x , y vector in equation (1) can be transformed into the circular cylindrical coordinate using the radial vector r ($x = r \cos \theta$ and $y = r \sin \theta$) and diffusion equation can be reconstructed as the following equation:

$$\frac{\partial C}{\partial t} = \frac{1}{r} \left\{ \frac{\partial}{\partial r} \left(rD \frac{\partial C}{\partial t} \right) + \frac{\partial}{\partial \theta} \left(\frac{D}{r} \frac{\partial C}{\partial \theta} \right) \right\} \quad (2)$$

here, since the chemical concentration is invariable in θ direction, the gradient toward the θ becomes zero. In steady-state, the diffusion equation at radial direction in the circular cylindrical coordinate can be given by following equation:

$$\frac{\partial C}{\partial t} = \frac{\partial}{\partial r} \left(rD \frac{\partial C}{\partial r} \right) = 0 \quad (3)$$

In fixed boundary condition, the equation (3) can be derived as follows:

$$C = \frac{C_1 \ln(b/r) + C_2 \ln(r/a)}{\ln(b/a)} \quad (4)$$

where C_1 is the initial concentration at $r = a$ and its value is 1, and C_2 is the final concentration at $r = b$ and its value is 0 (a and b is the initial and final position at the center chamber, respectively). Finally, in steady-state, the theoretical solution showed a good agreement with experimental results.

S.5 Device characterization using different pore size of membrane

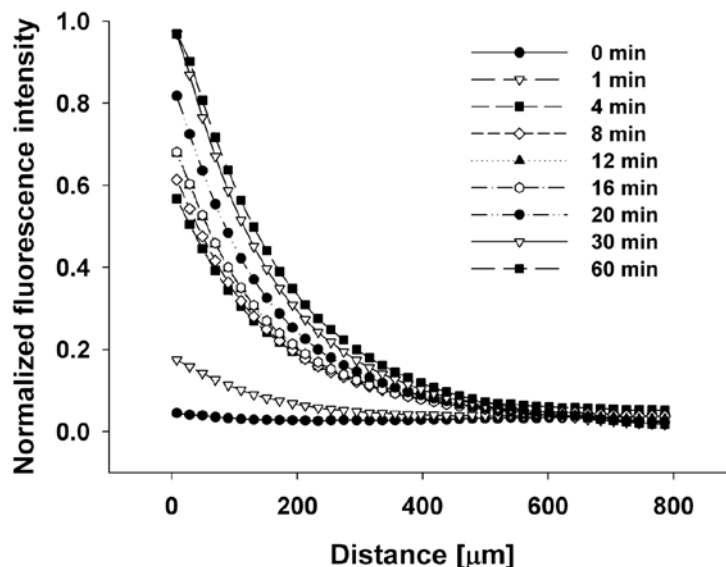


Fig. S4 Representative plots of the normalized FITC (90 °) fluorescent intensity profiles across the center channel as a function of time and steady-state gradients were established after 20 min.

We also tested the permeability of different pore size of membrane (silica nanospheres with 300 ± 15 nm diameter, Polyscience Inc., Warrington, USA) using a fluorescence dye. Three different of fluorescent dye were introduced into the each source channel at 90 ° for FITC, 210 ° for Rhodamine B, and 330 ° for Dylight 549. Subsequently, in order to maintain the solution concentration in the right and left channels, a flow rate of 4.0 $\mu\text{L}/\text{min}$ was controlled by withdrawing the solution. Finally, M9 medium was introduced into the center chamber. Since there is no net flow of M9 medium in the center channel, but permeation of the fluorescent dye through the membranes occurs, a stable concentration is established across the center channel. Fig. 3S shows the one of representative plots of the normalized FITC (90 °) fluorescent intensity profiles across the center channel as a function of time and steady-state gradients were established within 20 min.

S.6 Chemotactic responses toward different concentrations of aspartate

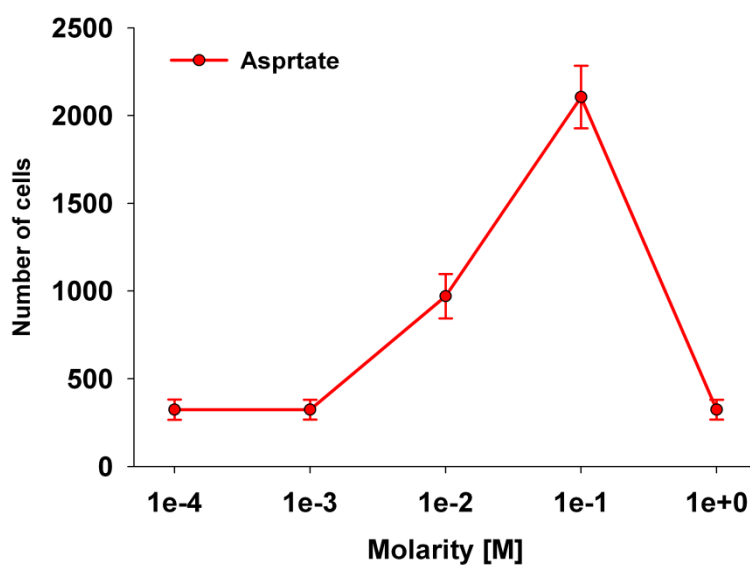


Fig. S5 Chemotactic responses toward different concentration of aspartate ranging from 10^{-4} M to 1 M.

Reference

1. E. L. Cussler, *Diffusion: Mass transfer in fluid systems*, Cambridge University Press, 2009.